Effect of terrestrial nutrient limitation on the estimation of the remaining carbon budget

Makcim De Sisto [1,2] and Andrew H. MacDougall [1]

[1]Climate and Environment, St. Francis Xavier University, Antigonish, NS, Canada
[2]Faculty of Engineering and Applied Science, Memorial University of Newfoundland, NL, Canada

Correspondence: Makcim De Sisto (mdesisto@stfx.ca)

Abstract.

The carbon cycle plays a foundational role in the estimation of the remaining carbon budget. It is intrinsic for the determination of the transient climate response to cumulative CO_2 emissions and the zero emissions commitment. For the terrestrial carbon cycle, nutrient limitation has a core regulation on the amount of carbon fixed by terrestrial vegetation. Hence, the addition of nutrients such as nitrogen and phosphorus in land model structures in Earth system models is essential for an accurate representation of the carbon cycle feedback in future climate projections. Thereby, the estimation of the remaining carbon budget is impacted by the representation of nutrient limitation in modelled terrestrial ecosystems, yet it is rarely accounted for. Here, we estimate the carbon budget and remaining carbon budget of a nutrient limited Earth system model, using nitrogen and phosphorus cycles to limit vegetation productivity and biomass. We use eight Shared Socioeconomic Pathways Scenarios (SSPs) and idealized experiments on three distinct model structures: 1) carbon cycle without nutrient limitation, 2) carbon cycle with terrestrial nitrogen limitation and 3) carbon cycle with terrestrial nitrogen and phosphorus limitation. To capture the uncertainty of the remaining carbon budget, three different climate sensitives were tuned for each model version. Our results show that overall the nutrient limitation reduced the remaining carbon budget for all simulations in comparison with the carbon cycle without nutrient limitation. Between the nitrogen and nitrogen-phosphorus limitation, the latter had the lowest remaining carbon budget. The mean remaining carbon budget from the Shared Socioeconomic Pathways scenarios simulations for the 1.5 °C target in the no nutrient limitation, nitrogen limited and nitrogen-phosphorus limited models obtained were 228, 185 and 175 Pg C respectively, relative to year 2020. For the 2 °C target the mean remaining carbon budget were 471, 373 and 351 Pg C for the no nutrient limitation, nitrogen limited and nitrogen-phosphorus limited models respectively, relative to year 2020. This represents a reduction of 19 and 24 % for the 1.5 °C target and 21 and 26 % for the 2 °C target in the nitrogen and nitrogen-phosphorus limited simulations compared to the no nutrient limitation model. These results show that terrestrial nutrient limitations constitute an important factor to be considered when estimating or interpreting remaining carbon budgets and are an essential uncertainty of remaining carbon budgets from Earth system model simulations.

1 Introduction

Future climate projections have only rarely accounted for nutrient limitation of the land carbon sink (Wang and Goll , 2021). For the sixth phase of the Coupled Model Intercomparison Project (CMIP6) this weakness was partially overcome with more Earth system models (ESMs) embracing nitrogen limitation as a standard for terrestrial system structures. However, the inclusion of phosphorus remains rare and representation of micro-nutrients remains a distant ambition. (Arora et al. , 2020; Spafford and MacDougall , 2021). Thus, the future of the land carbon sink remains uncertain as projecting the interactions between the terrestrial system and atmosphere is a challenge without fully accounting for nutrient limitations (Achad et al. , 2016). Since year 1850, the cumulative CO_2 land sink has been estimated to be 210 ± 45 PgC, which represents 31% of all anthropogenic carbon emissions (Friedlingstein et al. , 2022). The terrestrial carbon sink has increased historically with increasing CO_2 emission rate, such that the proportion of carbon taken up by land has remained close to constant (Friedlingstein et al. , 2022).

Nutrient availability constrains the capacity and rate at which terrestrial plants assimilate carbon (Goll et al. , 2012). Nitrogen and phosphorus are the nutrients that most commonly limit vegetation growth (Filipelli , 2002; Fowler et al. , 2013; Wang et al. , 2010; Du et al. , 2020) and hence have been the subject of most research and large scale modelling efforts. Globally, this effect varies. Most of the terrestrial biosphere is co-limited by both N and P, with N being the dominant nutrient limitation in higher latitudes while phosphorus predominates in lower latitudes (Du et al. , 2020). Earth system models are designed to account for land use change, and biological productivity when estimating the carbon sink on land (Kiwamiya , 2020). The change of nutrient concentration in terrestrial systems in future simulations is an uncertainty for determining the land carbon sink over the next decades (Shibata et al. , 2010, 2015; Menge et al. , 2012). Complicating this problem further, a large portion of nutrients on land are derived from anthropogenic sources, including agricultural fertilization (artificial, compost and manure), atmospheric deposition of N-bearing pollutants, and urban wastewaters (Lu and Tian , 2017; van Puijenbroek et al. , 2019).

It is likely that the first generation of ESMs simulations overestimated how much terrestrial ecosystems would respond to an increase in atmospheric carbon dioxide concentrations based on carbon only schemes (Wieder et al. , 2015). A large amount of terrestrial carbon uptake was predicted by those simulations, which would result in unrealistic nutrient requirements. For example, in a study by Wieder et al. (2015) ESMs with nitrogen and nitrogen–phosphorus limitation were projected to decrease net primary productivity by 19% and 25%. Hence, the implementation of nutrient limitation in ESMs has been shown to improve the representation of carbon uptake in land (Wang et al. , 2007, 2010; Goll et al. , 2017; De Sisto et al. , 2022), and thus will effect the carbon budget.

The carbon budgets can be seen from two perspectives. The first describes pools and fluxes of carbon within the Earth system (Friedlingstein et al. , 2022). This perspective serves to understand how natural sinks respond to changes in climate, CO_2 and CH_4. The second, is the remaining carbon budget, that describes the allowable future CO_2 emissions to reach a temperature target, commonly 1.5 and 2 °C, which is derived from another metric, the transient climate response to cumulative CO_2 emission (TCRE) which quantifies how global surface temperatures are nearly proportional to cumulative CO_2 emissions (Matthews et al. , 2009; MacDougall , 2016; Spafford and MacDougall , 2020). As TCRE represents the proportionality of cumulative CO_2 emission to its accompanying temperature change, its inverse can be use to estimate the remaining carbon budget for

temperature targets (Matthews et al. , 2020). The TCRE have been shown to be a good metric for predicting the response of temperature to cumulative CO_2 emissions. However, the TCRE only represented warming from CO_2 emissions, excluding the impacts of non-CO_2 forcing agents. A method to account for this issue is to use simulations with all anthropogenic forcing and plot the total anthropogenic warming as a function of cumulative CO_2 emissions, also known as effective TCRE (Tokarska et al. , 2018). There is a large uncertainty in the TCRE estimates, with a likely range from 1.0 to 2.3 K EgC^{-1} (IPCC , 2021). For idealized experiments the Transient Climate Response (TCR) can be used to quantify the physical uncertainty in TCRE. TCR is the amount of global warming expected to occur when atmospheric CO_2 concentrations double from their pre-industrial levels, while all other factors remain constant. This corresponds to year 70 in a 1pctCO2 experiment where the annual CO_2 concentration is increased at a rate of 1 % yr^{-1} (Eyring et al. , 2016). The TCR is dependent on rates of CO_2 concentrations represented in the input datasets. However unlike TCRE, the TCR is dependent on the scenario used to compute it (e.g. Mac-Dougall (2017)). The other important source of variability among TCRE estimates comes from uncertainties in carbon taken up by the ocean and terrestrial biosphere.

Terrestrial system nutrient limitation play a vital role in the estimations of remaining carbon budgets due to their effect on the carbon cycle. Accounting for phosphorus limitation in carbon budgets estimations is desirable due to for its limiting effect at low latitudes (Du et al. , 2020). Hence, P impact on terrestrial vegetation biomass and limitation of carbon sink almost certainly affect remaining carbon budget estimates. This study assesses how nutrient limitation affects several uncertainties in remaining carbon budget estimates, including uncertainty in the TCRE, the estimated contribution of non-CO_2 climate forcings to future warming, the correction for the feedback processes presently unrepresented by Earth System Models, and the unrealized warming from past CO_2 emissions–called the zero emissions commitment (ZEC) (Rojelj et al. , 2018). In addition to these four factors knowledge of the human-induced warming to date is needed to compute the remaining carbon budget. This value is well estimated from historical records (Arias et al. , 2021). Nutrient limitation can be used to improve historical warming accuracy in emission forced ESMs simulations (De Sisto et al. , 2022). The TCRE represents the response of temperatures to CO_2 emissions, hence different models can represent different remaining carbon budgets based on different carbon-climate sensitivities. The non-CO_2 emissions affect the change of temperatures and need to be understood to maintain desired temperature targets. Morever, the change in temperature after emission cessation is an important dynamic that should be understood and considered in remaining carbon budgets estimations. In future projections non-CO_2 climate forcings are likely affected by the introduction of nutrient limitation in ESMs. The main impacts include feedback changes due to land carbon sink and land use change emissions variation (including albedo changes), either by photosynthesis limitation or the reduction of terrestrial vegetation biomass. These changes might also impact the expected warming contribution after CO_2 emissions are ceased. Lastly within this remaining carbon budget framework, N and P constitute an unrepresented source of Earth system feedbacks that now is accounted in the present simulations.

Isolating the effects of N and P terrestrial limitation give a novel insight on how underrepresented process in terrestrial systems contribute to remaining carbon budgets uncertainties. It is therefore important to understand how ESMs carbon cycle sensitivity to nutrient limitation constrain of the land carbon sink in future simulations. Hence, we explore the effect of ter-

restrial nitrogen and phosphorus limitation in remaining carbon budget estimates in an intermediate complexity Earth system model under historical, idealized, and Shared Socioeconomic Pathways projections.

2 Methodology

2.1 Model description

95 Simulations to quantify the remaining carbon budgets were carried with the University of Victoria Earth System Climate Model (UVic ESCM). The UVic ESCM version 2.10, is a global intermediate complexity model (Weaver et al. , 2001; Mengis et al. , 2020). The model is comprised of a 3D dynamic ocean circulation model (Pacanowski , 1995), along with a simplified moisture-energy balance atmosphere (Fanning and Weaver , 1996), a dynamic-thermodynamic sea ice model (Bitz et al. , 2001) and a land surface model (Meissner et al. , 2003).

100 In the model, the terrestrial and oceanic carbon cycle are represented. The ocean comprises 19 vertical levels that become thicker with depth (50 m near the surface to 500 m in the deep ocean). Ocean biogeochemistry is based on a simple nutrient-phytoplankton-zooplankton-detritus model (Keller et al., 2012; Schmittner et al., 2005), with representation of ocean carbonate chemistry and sediments (Mengis et al. , 2020).

In the 2.10 version of the model, the soil is represented by 14 subsurface layers with their thickness increasing exponentially
105 with depth, with the surface layer measuring 0.1 m, the bottom layer measuring 104.4 m, and the total layer measuring 250 m. Hydrological processes are active in the first eight soil layers (top 10m), while the layers below have granitic characteristics. The soil carbon cycle is active up to a depth of 3.35 m (6 layers) (Avis , 2012; MacDougall et al. , 2012). TRIFFID (top-down representation of interactive foliage and flora including dynamics) represents vegetation interaction between 5 functional plant types within the terrestrial vegetation. Based on the Lotka-Volterra equations (Cox , 2001), broadleaf trees, needleleaf trees,
110 shrubs, C3 grasses, and C4 grasses compete for space in the grid. Appendix C1 shows the representation of above ground vegetation biomass compared to Santoro et al. (2024) dataset. Through photosynthesis, carbon is uptake and allocated to growth and respiration, whereas the vegetation carbon is transferred to the soil through litter fall and allocated to the soil in a decreasing function of depth. Permafrost carbon is prognostically generated within the model using a diffusion-based scheme meant to approximate the process of cryoturbation (MacDougall and Knutti , 2016).

115 The UVic ESCM prescribes anthropogenic land-use changes based on standardized CMIP6 land-use forcing (Ma et al., 2020) regridded to the UVic ESCM grids. Land-use data products have been modified for UVic ESCM use by aggregating cropland and grazing land into one crop type, representing any of the five functional types of crops, and one grazing variable, representing pastures and rangelands. By using this forcing, the model determines the fraction of grid cells that contain crops and grazing areas, and these fractions are assigned to C3 and C4 grasses and excluded from the vegetation competition routine
120 of TRIFFID. Land use change emissions releases 50% of the carbon stored in vegetation directly to the atmosphere when forest or other vegetation is cleared from croplands, range lands or pastures. The remaining 50% remains in a short-lived soil carbon pool. A full description of the model can be found in Mengis et al. (2020).

A terrestrial nitrogen and phosphorous model has recently been developed for the UVic ESCM (De Sisto et al. , 2022). The nitrogen cycle module consists of three organic pools (litter, soil organic matter, and vegetation) and two inorganic pools
125 (NH_4^+ and NO_3^-). Nitrogen input is represented by atmospheric nitrogen deposition and biological nitrogen fixation. The latter is dependent on the terrestrial Net Primary Productivity (NPP). Biological nitrogen fixation and mineralization of organic

nitrogen produce NH_4^+, which can be absorbed by plants (vegetation), leached, or transformed into NO_3^- via nitrification. NO_3^- is produced through nitrification, can be taken up by plants, leached or denitrified into NO, N_2O or N_2. Inorganic N is distributed between leaf, root, and wood, with wood having a fixed stoichiometric ratio and leaf and root pools having a variable ratio. The partition of carbon, nitrogen and phosphorus among plant structures does not change in when the soil is considered to be nutrient limited. Organic N leaves the living pools via litter-fall into the litter pool which is either mineralized or transferred to the organic soil pool, part of this N can be mineralized into the inorganic N pools. Before litterfall, a constant fraction of the N is reabsorbed. Mineralization of the litter and organic matter pool is dependent on turnover rates, concentration of nitrogen, soil temperature and soil moisture. At the same time N can flow from the inorganic to the soil organic pool via immobilization. A complete description of the nitrogen cycle can be found in Wania et al. (2012) and De Sisto et al. (2022).

The phosphorus module includes three inorganic (labile, sorbed and strongly sorbed) and three organic P pools: Vegetation (leaf, root and wood), litter and soil organic P. The P input is driven by a fixed estimates of P release per global soil types as in Wang et al. (2010). Inorganic P (P_{soil}) in soil follows the dynamics described in Goll et al. (2017) where a fraction of the inorganic soil phosphorus is transfered to the sorbed pool while the remaining fraction is consired to be labile. A portion of the sorbed pool is also transfered to the strong sorbed pool where it is considered a loss of phosphorus from the soil system. After uptake, P is distributed in three vegetation compartments: leaf, root and wood. Leaf and root have a dynamic value that varies between a minimum and a maximum, while wood have a fix C:P ratio. The vegetation P biomass dynamics are determined from the difference between the amount of uptake and the loss from litterfall. Before littefall, a fraction of phosphorus is reabsorbed. The litter P pool is dependent on three terms: the input from litterfall, the decomposition rate and loss from mineralization (Wang et al. , 2007). The soil litter decomposed is transferred to the soil organic P pool. The mineralization of phosphorus is determined from the maximum rate of P mineralization, the N cost of plant root P uptake, a critical value of N cost for root P uptake from where phosphatase production begins and a Michaelis-Menten constant for P mineralization. A complete description of the P cycle can be found in De Sisto et al. (2022).

Nitrogen and phosphorus limit terrestrial vegetation growth in the model in two different ways: 1) Nitrogen limits the photosynthetical activity (by regulating the maximun carboxilation rate of RuBISCO) and directly by reducing biomass. This reduction is controlled by the maximum C:N leaf ratio, where reducing this value corresponds to a larger reduction of vegetation biomass. 2) A stoichiometric reduction of biomass when N and P are considered to be limiting terrestrial plants. If C:N ratios are above a set ratio threshold, wood and root carbon biomass are then transferred to the litter pool (reassembling decaying vegetation when in nutrient limiting environments) until the "normal" set C:N ratio is reached. There is no direct inclusion of P limitation in photosynthesis-related equations. Past model development efforts tested different approaches such as Walker et al. (2014) but the concepts were incompatible with the current version of land vegetation model structure.

2.2 Experimental set-up

The effects of nitrogen and phosphorus were analysed from the perspective of the sources of uncertainty in the remaining carbon budgets estimates. Here, the framework includes how nitrogen and phosphorus impact the representation of: 1) Model fidelity of human warming to date, 2) the TCRE, 3) the unrealized warming from past CO_2 emissions (zero emissions commitment)

and, 4) the estimated contribution of non-CO_2 climate forcings to future warming. We run three different versions of the UVic ESCM version 2.10: 1) Carbon only (C-only), 2) Carbon Nitrogen (CN) and Carbon Nitrogen and Phosphorus (CNP). Furthermore, to capture the uncertainty of the carbon budget estimates, the equilibrium climate sensitivity was tuned by using a parameter designed by Zickfeld et al. (2009) to alter climate sensitivity in the UVic ESCM by altering the flow of long-wave radiation back to space. The dynamics of the alteration is represented in the following equation:

$$L_{out}^* = L_{out} - c(T - T_0), \tag{1}$$

where L_{out}^* is the modified longwave radiation, L_{out} is the unmodified longwave radiation, c is a proportionality constant that corresponds to specific equilibrium climate sensitivities, T is the present global average temperature and T_0 is the global average temperature at the initial year of the simulation. The parameter c is used to increase or decrease the net climate feedback by reducing or increasing the outgoing longwave radiation. Model variants were tuned to have Equilibrium Climate Sensitivities (ECSs) per doubling of CO_2 of 2.0°C, 4.5°C to represent the "likely bounds" (IPCC , 2021), as well as using the emergent climate sensitivity of the model (3.4°C) as the central estimate.

2.2.1 Historical human-induced warming to date

We conducted three historical simulations to assess the historical climate response differences between the C-only and CN and CNP. Each model structure was calibrated using aerosol scaling so that historical temperatures match observations. We used Goddard Institute for Space Studies (GISS) temperature observations in this study. Three-dimensional aerosol optical depth can be scaled by a fraction in the UVic ESCM and was used in version 2.10 to calibrate aerosol forcing to fit current values (Mengis et al. , 2020). Thus the historical warming to date is similar for all model variants but the estimated historical emissions vary, allowing model validation. The non-CO_2 forcing included solar, volcanic, aerosol and the aggregate forcing from halocarbons, CH_4, and N_2O.

2.2.2 Transient climate response to cumulative emissions

To diagnose the TCR and the TCRE, we run simulations starting with a 1% yr^{-1} increase in CO_2 concentrations until a doubling and quadrupling(2x and 4xCO_2) were reached after which the concentration was kept constant (Eyring et al. , 2016). Both TCR and TCRE are computed at year 70 of this 1pctCO_2 experiment, when atmospheric CO_2 concentration has doubled. To account for non-CO_2 forcing effect on climate sensitivity, we applied (Tokarska et al. , 2018) approach to compute effective TCRE. This approach uses Share Socioeconomic pathways (SSPs) projections to simulate a full forced simulation. The SSPs represent different futures that represents a wide array of climate outcomes. For the effective TCRE, SSP 5-8.5 is used to represent a full forced simulation to estimate the response of temperature to cumulative emissions

2.2.3 Zero emissions commitment

To explore the effects of nutrient limitation on zero emission commitment, an experiment was done following the protocol of the Zero Emission Commitment Model Intercomparison Project (ZECMIP). The objective of ZECMIC is to quantify the amount of unrealized temperature change after CO_2 emissions have ceased and the drivers behind the change (Jones et al. , 2019). The experimental protocol was applied to C-only, CN and CNP. For these experiments the 1pctCO2 experiment is followed until diagnosed cumulative emissions of CO_2 reaches 1000 PgC thereafter emissions are set to zero further CO_2 emissions. We diagnosed three emissions pathways corresponding to C-only, CN and CNP simulations. We used two metrics to assess the nutrient limitation effect on ZEC. The first, is the temperature at the 50th year after emission have ceased relative to the global average temperature when emissions ceased, averaged from year 40 to year 59 after emissions cease (ZEC$_{50}$) as in MacDougall et al. (2020). The second, is the mean ZEC for 100 years after emission have ceased.

2.2.4 Estimated contribution of non-CO$_2$ climate forcings to future warming

To estimate the impact of nutrient limitation on the contribution of non-CO$_2$ climate forcings to future warming, eight SSPs scenarios for the C-only, CN and CNP version of the UVic ESCM version 2.10 were run. We included the CMIP6 SSPs array scenarios representing each distinct future (1-5) narrative. The following scenarios were run: SSP1-1.9, SSP1-2.6, SSP2-4.5, SSP3-7.0, SSP4-3.4, SSP4-6.0, SSP5-3.4-OS and SSP5-8.5. The carbon budget follows temperature anomalies normalised to 1850-1900 mean for 1.5, 2, 2.5 and 3 °C targets. For the four overshoot scenarios (SSP1-1.9, SSP1-2.6, SSP4-3.4, and SSP5-3.4-OS) the remaining carbon budget is computed for the time when the target is first breached.

To estimate the effect of nutrient limitation in land use change emissions and terrestrial albedo an extra set of three simulations for C-only, CN and CNP and the same eight SSP scenario simulations where conducted. In these simulations land use change forcing was set to the pre-industrial year 1850 value. The model adjusts its diagnosed CO_2 emissions to account for the missing land use change forcing. Hence, the diagnosed emission difference between the simulations with land use change forcing and without forcing corresponds to the estimated amount of land use change emissions (Mengis et al. , 2018). These values also carry the effect of albedo change due to land use change. Hence, our values show the total land use change emission + albedo effect simulated in the model.

3 Results

3.1 Historical human-induced warming to date

215 For each model structure the historical temperature was calibrated to match historical observations by altering the efficacy of aerosol forcing. Figure 1 shows the resulting near-surface air temperature anomalies for UVic ESCM C-only, CN, and CNP configurations after calibration relative to 1951-1980 climate normal. The temperature anomalies were plotted against GISS near surface air temperatures anomalies relative to 1951-1980 (GISTEMP Team , 2023). For the three different versions of the model the resulting calibrated simulations reproduced well the historical temperature trend when compared to GISS

220 observations. As shown in De Sisto et al. (2022) without calibration the UVic ESCM CN and CNP have higher temperatures when compared to C-only, given that nutrients limit the capacity of the terrestrial system to take up atmospheric CO_2. That is, atmospheric CO_2 is higher given the same total emissions of CO_2. Between CN and CNP, CNP results in higher temperature response mainly as a result of tropical terrestrial nutrient limitation and extra phosphorus limitation in higher latitudes.

Figure 2 shows the historical global carbon cycle from 1850-2021 for C-only, CN and CNP. There are two main impacts of

225 nutrient limitation on terrestrial systems: 1) reduction of the land carbon sink and 2) reduction of the land use change emissions. The reduction of the land carbon sink is related to the decrease of the photosynthetic capacity and the regulation of terrestrial vegetation biomass. This biomass reduction leads to the reduction of the land use change emissions, especially as N and P affects woody biomass greatly. The global reduction of carbon uptake increase the concentration of CO_2 in emission driven simulations. Following this logic and given that concentration driven simulation have a set atmospheric CO_2 concentrations, the

230 diagnosed emissions estimated in our simulations were reduced in CN and CNP compared to C-only. The model estimates less emissions to be necessary to keep the CO_2 concentration on track as less carbon is taken up from land. In order to be comparable to the latest carbon budget report out estimation of the historical carbon cycle follows carbon fluxes from 1850-2021 while the estimation of the remaining carbon budgets starts from the year 2020 following different future SSPs scenarios pathways. From 1850-2021 (Figure 2) the range of reduction in the CN and CNP nutrient limited simulations for the cummulative land

235 carbon sink was 75 to 106 Pg C compared to C-only. The range of reduction for cummulative the land use change emission was 60 to 93 Pg C. Finally, the range of reduction of the cumulative carbon emissions diagnosed by the concentration driven simulations was 11 to 29 Pg C. The CNP cumulative fossil fuel CO_2 emissions of 483 PgC is within the value of 465$\pm$25 PgC given by Friedlingstein et al. (2022) while C-only and CN are slightly over the estimate with 501 and 512 PgC (Figure 2).

3.2 Transient climate response to cumulative CO_2 emissions

240 The TCR for doubling CO2 concentrations was 1.78, 1.79 and 1.79 °C in C-only, CN and CNP. These small differences are driven by albedo changes. Between CNP and CN, the albedo change has a small increase effect of 0.004 °C in CNP compared to CN (note the UVic ESCM lacks internal variability, so this very small difference is computable). The TCRE for C-only resulted in 1.74 K EgC^{-1} compared to CN 1.94 K EgC^{-1} and CNP 2.07 K EgC^{-1}. The TCRE values for all the simulations are within the range of 1 - 2.3 K EgC^{-1} given by the IPCC AR6 Summary for Policy Makers (IPCC, 2021). Under a 1%

245 atmospheric CO_2 increase per year experiment, terrestrial nutrient availability limits the capacity of terrestrial vegetation to

uptake carbon. Hence, even with a rapid increase of CO_2 concentration in the atmosphere, terrestrial vegetation carbon uptake capacity is limited, and the uptake rates are not as high as with an unlimited amount of nutrients readily available for uptake. The effective TCRE estimated from SSP5-8.5 resulted in 1.97, 2.27 and 2.36 K EgC $^{-1}$ for C-only, CN and CNP. Overall the TCRE and effective TCRE were increased in the nutrient limited simulations. The range of increase for TCRE was: 0.2

250 to 0.3 K EgC $^{-1}$. The range of increase of the effective TCRE was: 0.3 to 0.4 K EgC $^{-1}$. Figure 2 shows how terrestrial carbon cycle fluxes change in historical simulations. Due to these changes the diagnosed CO_2 emissions are reduced, hence, for any temperature target less CO_2 emissions need to be emitted in the nutrient limited simulations. This translates into a more sensitive model, where for 1000Pg C emitted the nutrient limiting simulations are going to result in higher temperatures.
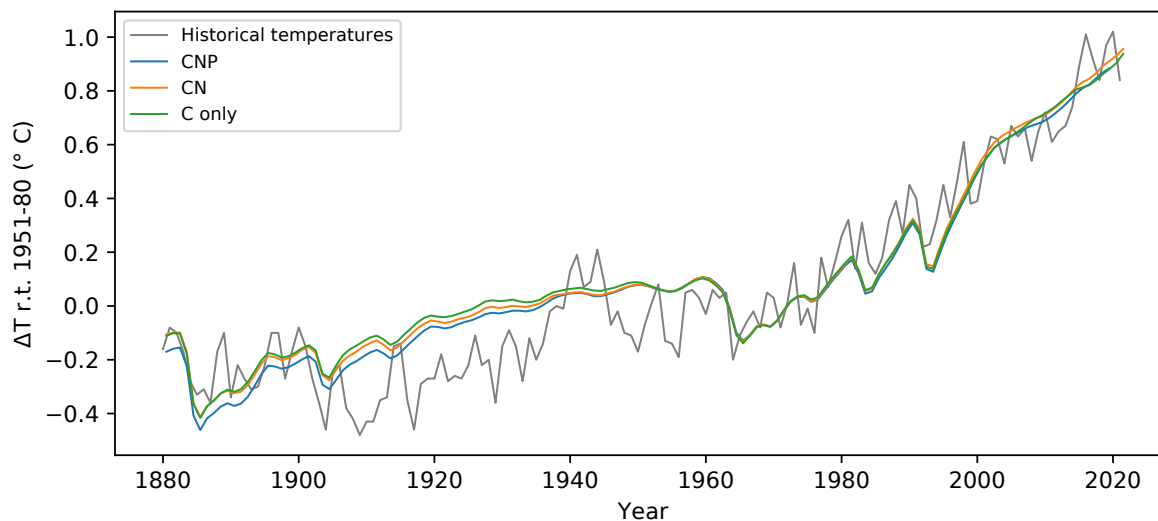
Figure 1. Historical temperature relative to 1951-1980 of C-only, CN and CNP compared to GISS historical temperature dataset (GISTEMP Team , 2023).
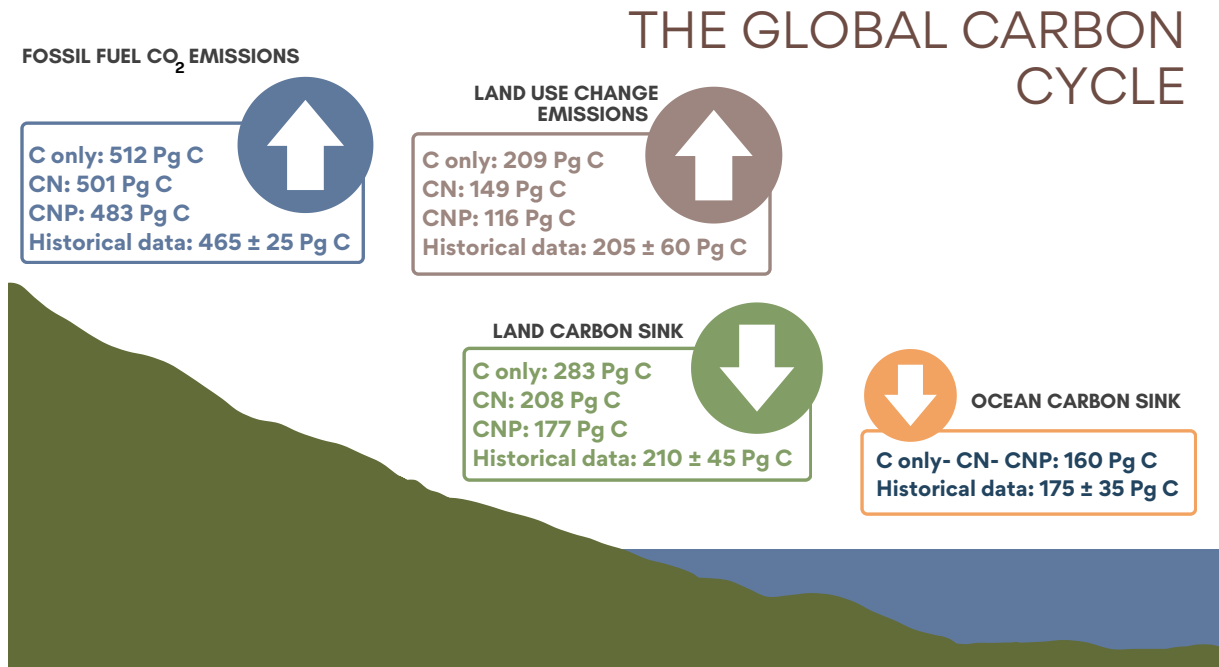
Figure 2. Historical 1850-2021 cummulative land carbon sink, ocean sink, land use change emissions and diagnosed CO_2 emissions simulated compared to Friedlingstein et al. (2022).

3.3 Zero Emission Commitment

To analyse the impact of nutrient limitation in zero emission scenarios, ZECMIP type experiments were conducted in C-only, CN and CNP. Figure 3 show the temperature anomaly relative to the estimated temperature at the year of cessation. The temperature pattern in the 100 years following cessation is similar for all the model structures. There is an initial rise of temperature around the 20th year and a quick decline on the 35-40th year, followed by an increase around the 70-80th year. A difference between C-only and CN and CNP is that the C-only simulation increase is lower than the nutrient limited simulations.The overall ZEC value is higher in CNP and CN than in C-only. Higher ZEC values indicate a larger increase of temperature after emissions have ceased. For CN and CNP the ZEC_{50} value resulted in 0.07 and 0.09 °C compared to 0.02 °C in C-only. These values are similar to the ZEC_{50} of 0.03 °C shown in MacDougall et al. (2020) for the same model. The ZEC across 100 years of simulation after emission have ceased show a larger difference in temperature change after emission have ceased. C-only resulted in 0.05 °C compared to 0.17 °C in CN and 0.21 °C in CNP. This represent a relevant increase of temperature after emission have ceased in the nutrient limited simulations.

3.4 Estimated contribution of non-CO_2 climate forcing to future warming

In this section we assessed the remaining carbon budgets variability between different nutrient limitation model structures in the eight SSPs used in CMIP6. Furthermore, our emphasis was to show the role of N and P representation in remaining carbon budgets estimates from different future scenarios. Figures 2-8 show the resulting remaining carbon budgets for SSP 1-1.9, 1-2.6, 2-4.5, 3-7.0, 4-3.4, 4-6.0, 5-3.4 and 5-8.5. Among these projections not all reached the 1.5, 2, 2.5 and 3 °C targets. SSP1-1.9 and SSP1-2.6 only reached the 1.5 °C target, SSP 4-3.4 and SSP 5-3.4 only reached the 2 °C target, SSP 2-4.5 reached the 2.5 °C target and SSP 3-7.0, SSP 4-6.0 and SSP 5-8.5 reached the 3 °C target. The remaining carbon budgets estimates and the SSP temperatures anomalies can be seen in more detailed in Appendix A1, A2, A3 and B1. Overall, the application of nutrient limitation increased the TCRE and hence, decrease the carbon budget for all set targets. As expected, among CN and CNP simulation phosphorus limitation reduced the remaining carbon budgets. The mean remaining carbon budgets estimated among the SSPs simulations for ECS 3.4 [ECS 4.5 to ECS 2] in the C-only, CN and CNP for 1.5 °C target were: 228[31 to 291], 185[25 to 259] and 175[9 to 223] Pg C respectively. For the 2 °C target the mean remaining carbon budget were 471[205 to 554], 373[154 to 479] and 351[137 to 402] Pg C for the C, CN and CNP configurations respectively. The remaining carbon budgets for the 2.5 °C target were 719[378 to 869], 591[321 to 725] and 596[315 to 673] Pg C. Finally, the remaining carbon budgets for the 3 °C target were 974.4[546 to 1174], 798[460 to 986] and 796[467 to 920] Pg C. This represents a reduction of 19 and 24 % for the 1.5 °C target, 21 and 26 % for the 2 °C target, 18 and 17% for the 2.5 °C target and finally 18 and 19 % for the 3 °C target in CN and CNP compared to C-only.

One of the impacts of nutrient limitation is in the change of land use change emissions corresponding to the reduction and change of vegetation. We found that the mean land use change emission budget among SSPs simulation from year 2020 to the 1.5 °C target in the ECS 3.4[ECS 4.5 to ECS 2] were: 31[2 to 39], 20[2 to 40] and 13[1 to 23] Pg C for C-only, CN and CNP respectively (Figure 9). Corresponding to a reduction of 11.2 and 18.4 Pg C in CN and CNP compared to C-only.
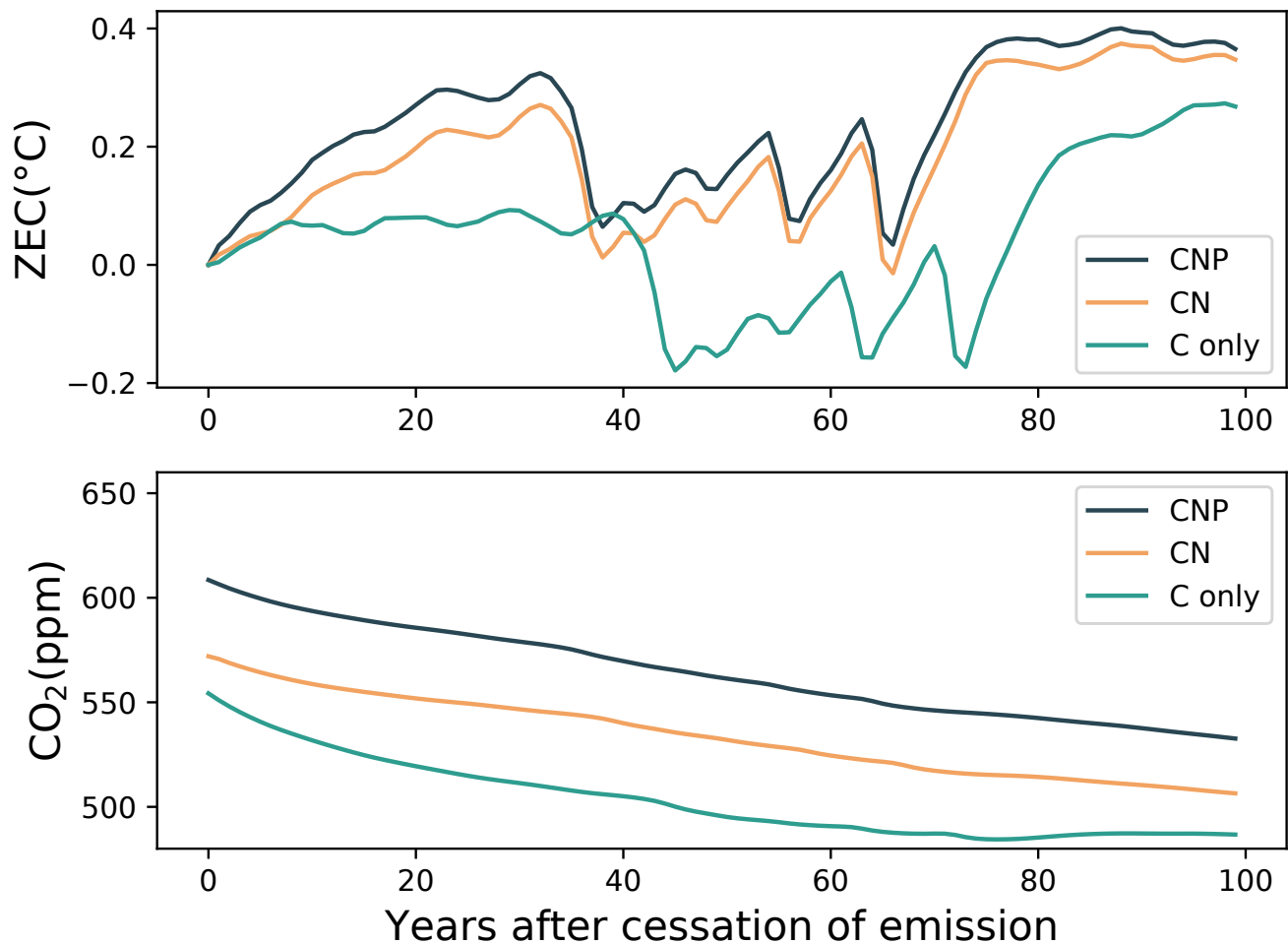
Figure 3. Zero Emissions Commitment following the cessation of emissions during the experiment wherein 1000 PgC was emitted following the 1pctCO2 experiment. ZEC is the temperature anomaly relative to the estimated temperature at the year of cessation. Note the UVic ESCM lacks internal variability. The rapid changes in global temperature seen in the top panel are due to disruptions to the ocean meridional overturing circulation (Mengis et al. , 2020)

These results demonstrate that the remaining carbon budget is clearly sensitive to the availability of nutrients represented in SSPs model simulations. As shown in figure 2,3,4,5,6,7 and 8 the remaining carbon budgets vary between the SSPs scenarios as temperature rise are effected by non-CO_2 forcings, corresponding to socioeconomical global uncertainties. Furthermore, the land carbon cycle in this case nutrient limitation, represents an implicit uncertainty under these different socioeconomical projections.
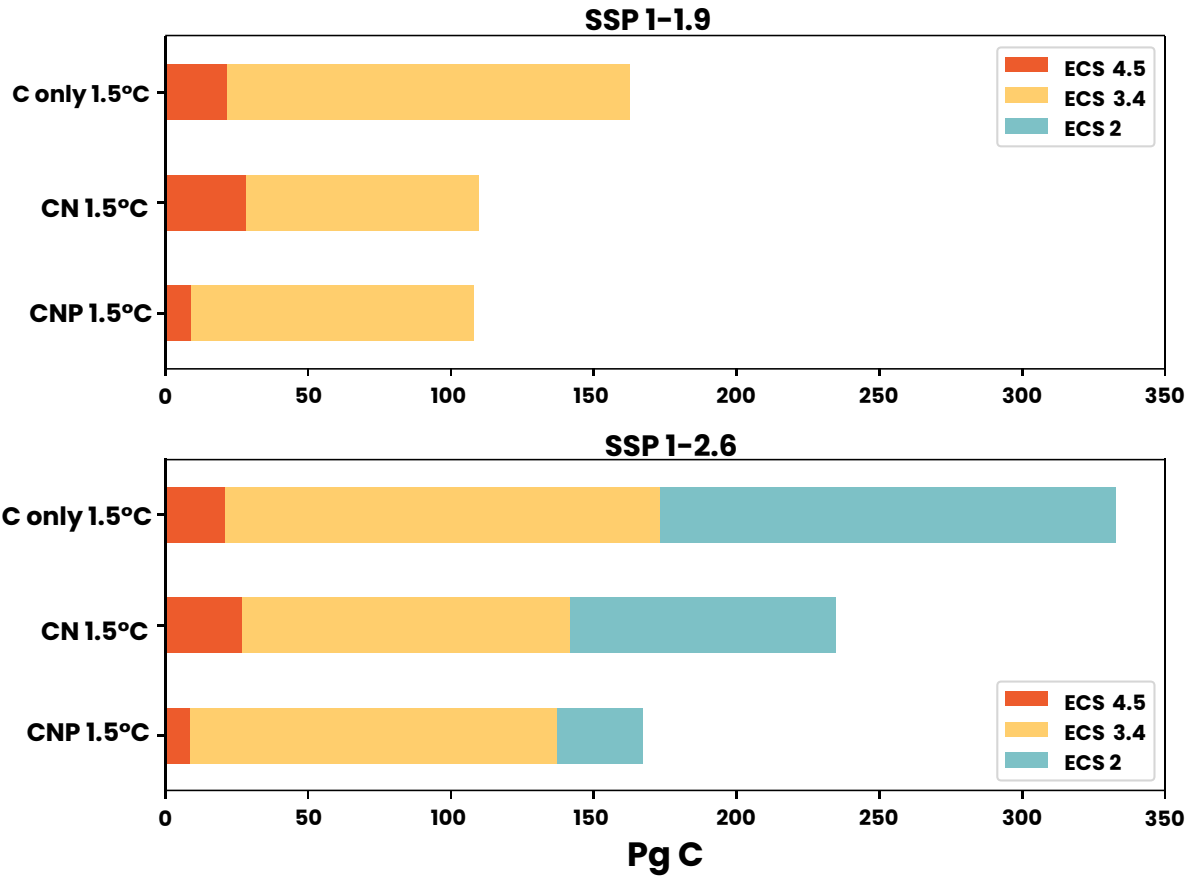
Figure 4. Carbon budgets for the 1.5 °C target for SSP 1-1.9 and 1-2.6. Three model sensitivities are shown as: ECS 4.5 dark blue, ECS 3.4 green and ECS 2 orange.
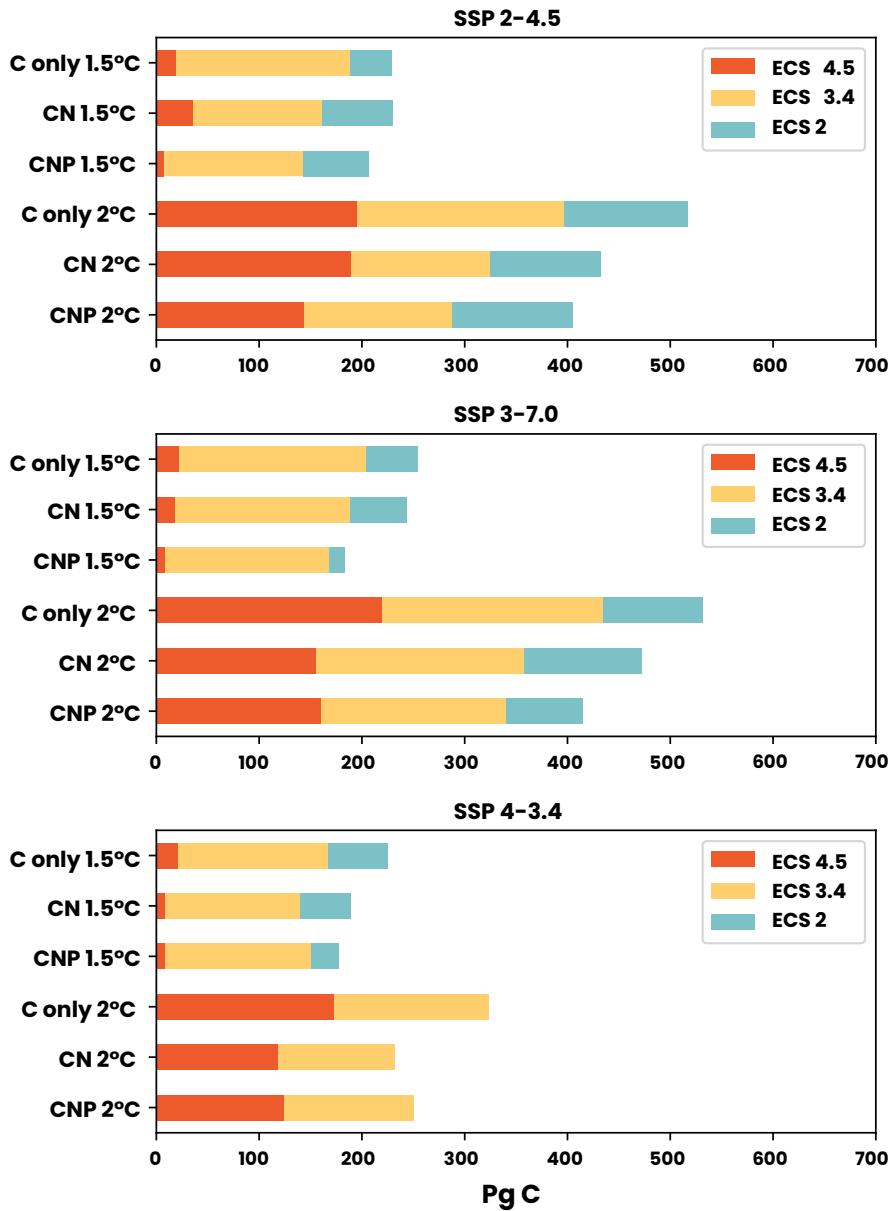
Figure 5. Carbon budgets for the 1.5 and 2 °C targets for SSP 2-4.5, 3-7.0 and 4-3.4. Three model sensitivities are shown as: ECS 4.5 dark blue, ECS 3.4 green and ECS 2 orange.
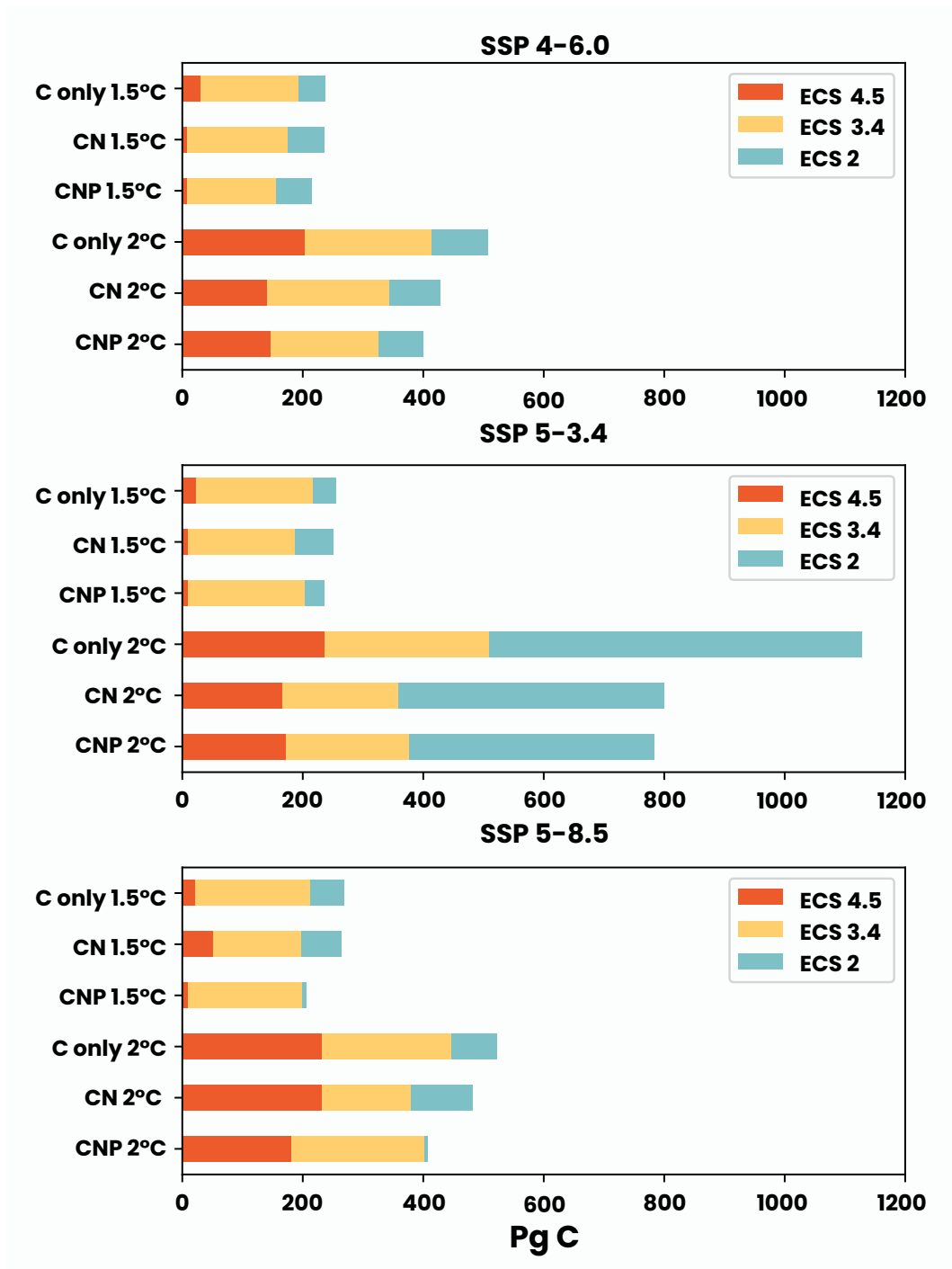
Figure 6. Carbon budgets for the 1.5 and 2 °C targets for SSP 4-6.0, 5-3.4 and 5-8.5. Three model sensitivities are shown as: ECS 4.5 dark blue, ECS 3.4 green and ECS 2 orange.
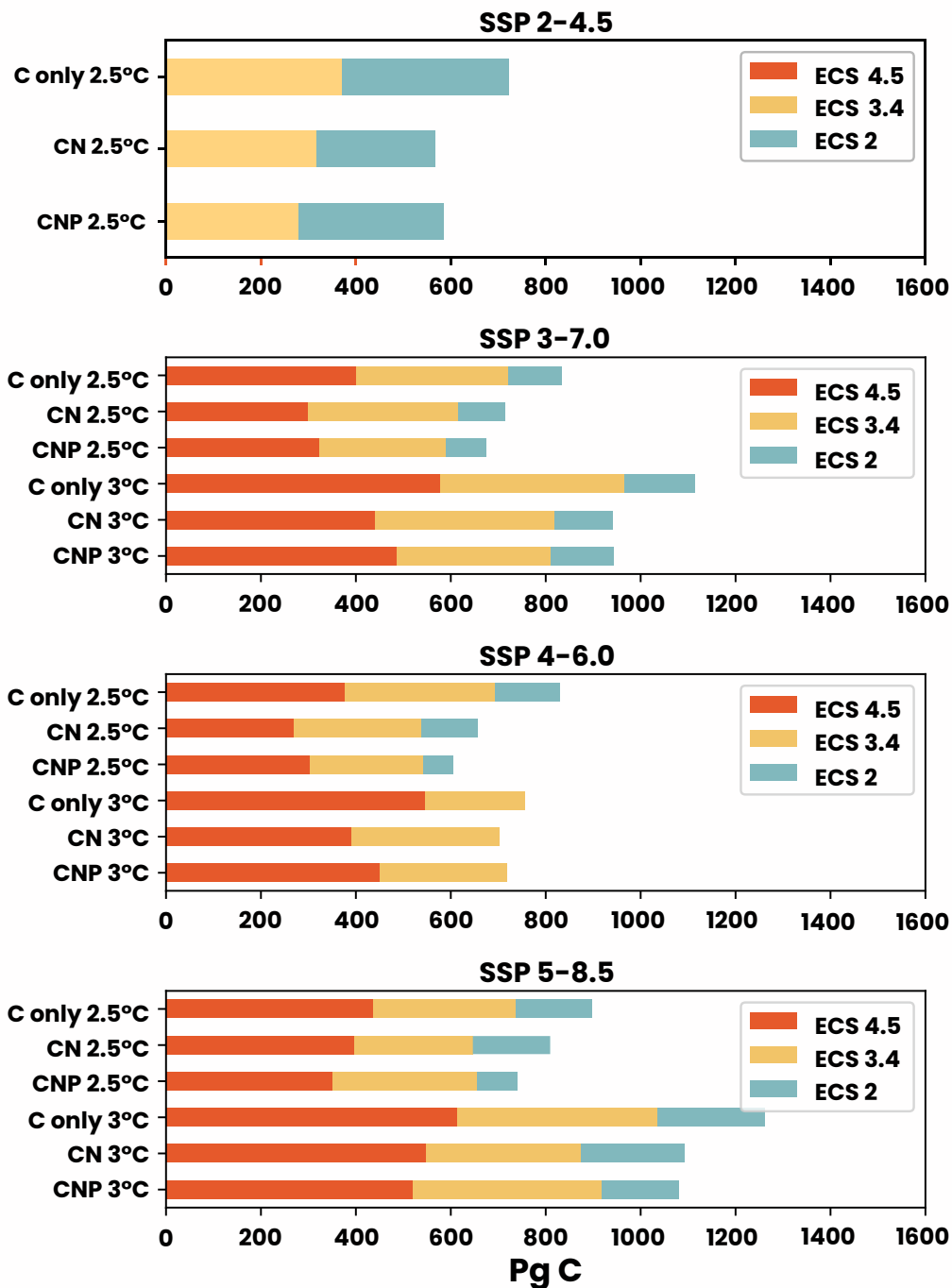
Figure 7. Carbon budgets for the 2.5, 3 °C targets for SSP 3-7.0, 4-6.0 and 5-8.5. These were the only scenarios that reached the targets. Three model sensitivities are shown as: ECS 4.5 dark blue, ECS 3.4 green and ECS 2 orange.
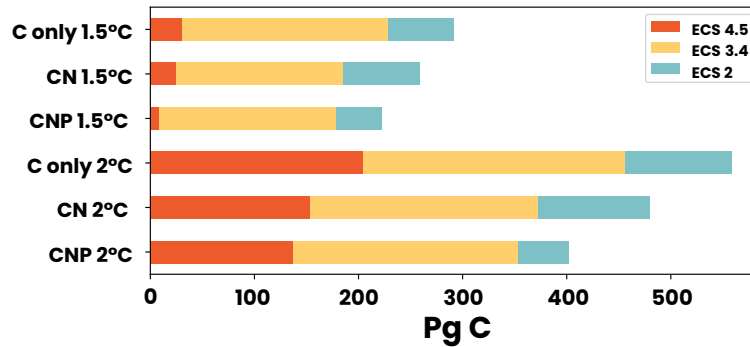
Figure 8. Mean SSP carbon budgets for the 1.5 and 2 °C temperature targets.
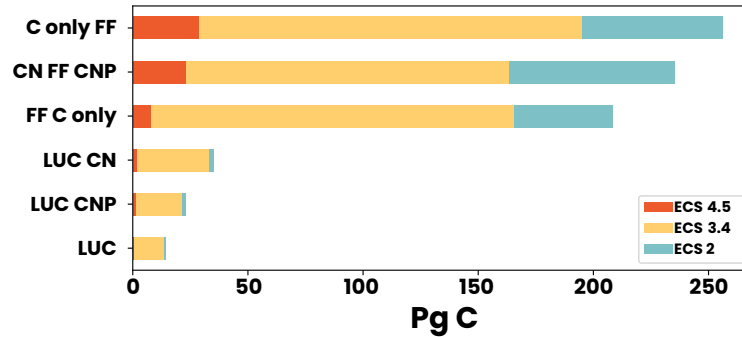
Figure 9. Mean SSP carbon budgets for Fossil Fuel (FF) and LUC emissions for the 1.5 °C temperature target.

4   Discussion

In nature N and P limitation or co-limitation has a core regulation on vegetation productivity. Hence, the inclusion of N and P limitation in ESMs improves the representation of vegetation productivity and biomass. In the UVic ESCM version 2.10, the vegetation biomass, distribution and productivity were addressed in (De Sisto et al. , 2022), while land use change emission and albedo remained unexplored. In this study, land use change emission account for albedo changes due to plant functional types changes in model simulations. As the model reduces vegetation due to nutrient limitation and trees are replaced by grasses, the land surface albedo is increased. The replacement of trees by grasses occurs globally in the model as shown in (De Sisto et al. , 2022). Hence, CNP and CN has a larger albedo value than C-only for land. We have identified that a terrestrial system

stressed with nutrient limitation reduces the land use change emissions budget and increases land surface albedo. The land surface albedo increased by 0.04 in nutrient-limited simulations.

The terrestrial carbon cycle in nutrient limiting model structures is usually suppressed by the capacity of primary producers to uptake carbon, either by controlling the photosynthesis or reducing the biomass directly by setting maximum nutrient ratios boundaries. In this case the terrestrial nitrogen and phosphorus act as a limiting factor for terrestrial vegetation by restricting the photosynthesis (N) and by reducing the biomass given a set ratio value (N and P). N and P control biomass directly by the maximum C:N or C:P leaf ratio threshold. The lower the set ratio is the higher impact will the nutrients have. When the diagnosed C:N or C:P leaf ratios are higher than the set maximum leaf ratio, the vegetation biomass dies so that the leaf ratios decrease back to the maximum ratio threshold. The nutrient limitation is also different for plant functional types and hence, the change in vegetation biomass is depended on differences among the limitation applied to each PFTs. Therefore, the application of multiple nutrient limiting stressors such as nitrogen and phosphorus should be applied carefully as a high limitation of phosphorus can easily underestimate the land sink capacity of tropical vegetation. A detailed description of the terrestrial nitrogen and phosphorus uncertainties can be found in the complete description of the model in De Sisto et al. (2022).

In CNP, biomass reduction goes beyond CN as tropical regions are subjected to more limitations. In the UVic ESCM 2.10, tropical regions have an overestimation of broadleaf trees in the tropics. When phosphorus is modelled, the result is a substantial decrease in land use change emissions compared to the base version of the model, leading to a substantial difference with Friedlingstein et al. (2022). However, CN is still within the range shown in Friedlingstein et al. (2022) study.

It is clear then that the representation of the carbon cycle in models structures affects the estimation of the remaining carbon budgets. Permafrost thawing for example has been studied for its carbon budget reduction effect in ESMs (MacDougall and Knutti , 2016; MacDougall et al. , 2021). In this study the effect of the terrestrial carbon dynamics has a direct impact on the reduction of the remaining carbon budgets. The impact of nitrogen and phosphorus limitation due to the reduction of the land carbon sink should be explicitly considered as a variable than can reduce our remaining carbon budgets for any temperature target. Furthermore, a significant number of socioeconomic uncertainties exist in the remaining carbon budget estimates, including the inability to predict future levels of carbon dioxide emissions based on sociopolitical system dynamics and technological advancements, such as the one represent in the different Shared Socioeconomic Pathways. Hence the carbon budgets are ultimately linked to the rate of emissions and the measures taken to mitigate carbon emissions in the future (Matthews et al. , 2020).

The IPCC AR6 (IPCC , 2021) reports remaining carbon budgets estimates from 2020 of 245, 177, 136, 108 and 82 PgC for the 1.5 °C target with a probability of 17, 33, 50, 67 and 83% respectively. Compared the 50% of probability of 136 PgC our nutrient limited model simulations, CN 185 PgC and CNP 175 PgC estimated a closer value than the C-only 228 PgC. C-only tending more to the 17% probability value. Hence, nutrient limited simulations brings the estimate from the UVic ESCM closer to the multi-model mean.

As shown in this study the representation of carbon processes can affect the estimation of remaining carbon budgets in ESMs. As unrepresented processes in other models, nitrogen and phosphorus limitation reduced the estimated remaining

carbon budget in CN and CNP by 43 and 53 PgC for the 1.5 °C target and 98 and 120 PgC for the 2 °C target when compared to the C-only simulation. These estimations are larger than the roughly estimate of 27 PgC reduction of carbon budgets due to unrepresented carbon feedbacks (Rojelj et al. , 2018), suggesting that this value may have been underestimated in the IPCC 1.5°C report.

The TCRE shows that nitrogen and phosphorus limitation had a direct effect on the temperature-to-carbon emission proportionality. The nutrient limitation impacts the carbon fluxes, reducing the land carbon sink and increasing the ocean carbon sink, leading ultimately to a net decrease of the carbon taken up from land and ocean. In emission-driven simulations, this will lead to a high buildup of atmospheric CO_2. However, it is clear that more understanding of nutrient distribution is necessary to build even more reliable nutrient-limited models. The effort should be directed towards the creation of reliable data including: global nutrient distribution, global nutrient inputs and future fertilization projections encompassing agriculture and human waste load into terrestrial, riverine and aquatic systems.

In ESMs, nutrient simulations could be improved with further global observations. The current available data have large ranges and make difficult to assess how reliable are the nutrient values given by ESMs simulations. Theses uncertainties are present in most aspects of the global nitrogen and phosphorus cycles. Hence, it is hard to grasp how accurate our model outputs are in comparison with nature. Especially in the case of phosphorus which lacks more observational datasets than nitrogen. Despite the uncertainty rooted in N and P models and projections, it is clear that nutrient limitation reduces the remaining carbon budgets by constraining the vegetation capacity in terrestrial ecosystems. Our results only show the effect of nutrient limitation in one model structure. The response of Earth system models to nutrient limitation varies amongst each other depending on how terrestrial nitrogen and phosphorus limitations are applied. Furthermore, although by varying ECS we may capture some of the range shown in other models, the full range of structural uncertainty is not captured by our experiment design.

The inclusion of P in ESMs and the benefits of CNP models has been shown to improve the accuracy of the the terrestrial carbon cycle (Wang et al. , 2010; Goll et al. , 2017; De Sisto et al. , 2022). However, the necessity of models of including P in their structures is debatable. If the objective is to improve the carbon cycle accuracy the inclusion of P is advisable for its limiting role in tropical regions. From a carbon budget estimations view, we observed similar results for CN and CNP. Overall, our results show that remaining carbon budgets estimated in CNP simulations were lower than CN. In SSPs were this was not the case, a medium or high land use regulation was implicit in the scenario. Hence, one of the main difference between CN and CNP models is how the model response to land use change management in different future projections scenarios. The inclusion of P in ESMs has been shown to improve the terrestrial model performance and hence, we believe that the addition of P limitation should be thought in the development plans of different model working groups.

5 Conclusion

Remaining carbon budgets are crucial for climate policy and management. As the remaining carbon budgets is intrinsically linked to the TCRE and the dynamics of the global carbon budget, it is important to consider the uncertainties that nutrient

limitation has on our terrestrial model structures. In this study we found that nutrient limitation, in this case N and P had a considerable effect on the remaining carbon budgets estimates. Historically, N and P limitation reduced the land carbon sink and land use change emission. The range of reduction of land carbon sink was: 75 to 106 Pg C and the range of reduction for the land use change emission was: 60 to 93 Pg C. Overall under the Shared Socioeconomic Pathways, N and P reduced the remaining carbon budgets estimates for 1.5, 2, 2.5 and 3 °C targets. CN and CNP showed a reduction of 43 and 53 Pg C for the 1.5 °C target and 98 and 120 Pg C for the 2 °C target respectively when compared to C-only. Theses values represent a reduction of 19 and 24 % for the 1.5 °C target, 21 and 26 % for the 2 °C target. After emission have ceased N and P had a relevant impact on the temperature change, the ZEC across 100 years of simulations after emission have ceased showed an increase in temperature for the nutrient limited simulations CN and CNP of 0.12 and 0.16 °C when compared to C-only. The uncertainty of the magnitude of the reduction in the remaining carbon budget from nutrient limitation will be more clear if a multimodel assessment is conducted. Overall we assess that accounting for nutrient limitations will lead to a substantial reduction in the estimated remaining carbon budget.

Table A1. Remaining carbon budgets from the Shared Socioeconomic Pathways: SSP 2- 4.5, 3- 7.0 and 4- 3.4 simulations for 1.5, 2°C targets relative to a warming from 1850-1900.

SSP scenarios	Target	Climate sensitivity	C-only(PgC)	CN(PgC)	CNP(PgC)
1- 1.9	1.5 °C	4.5	20	22	8
1- 1.9	1.5 °C	3.4	163	110	108
1- 1.9	1.5 °C	2	Not reached	Not reached	Not reached
1- 2.6	1.5 °C	4.5	21	27	9
1- 2.6	1.5 °C	3.4	173	142	137
1- 2.6	1.5 °C	2	332	235	167
2- 4.5	1.5 °C	4.5	21	37	9
2- 4.5	1.5 °C	3.4	189	161	144
2- 4.5	1.5 °C	2	231	231	208
2- 4.5	2 °C	4.5	197	191	144
2- 4.5	2 °C	3.4	397	325	288
2- 4.5	2 °C	2	516	433	406
3- 7.0	1.5 °C	4.5	23	19	9
3- 7.0	1.5 °C	3.4	204	189	170
3- 7.0	1.5 °C	2	255	244	184
3- 7.0	2 °C	4.5	220	155	161
3- 7.0	2 °C	3.4	435	359	343
3- 7.0	2 °C	2	532	473	416
4- 3.4	1.5 °C	4.5	22	9	- 9
4- 3.4	1.5 °C	3.4	168	141	150
4- 3.4	1.5 °C	2	226	190	178
4- 3.4	2 °C	4.5	174	119	125
4- 3.4	2 °C	3.4	324	233	250
4- 3.4	2 °C	2	Not reached	Not reached	Not reached

Table A2. Remaining carbon budgets from the Shared Socioeconomic Pathways simulations: SSP 4- 6.0, 5- 3.4 and 5- 8.5 for 1.5, 2°C targets relative to a warming from 1850-1900.

SSP scenarios	Target	Climate sensitivity	C-only(PgC)	CN(PgC)	CNP(PgC)
4- 6.0	1.5 °C	4.5	32	8	10
4- 6.0	1.5 °C	3.4	194	177	157
4- 6.0	1.5 °C	2	238	236	215
4- 6.0	2 °C	4.5	174	119	125
4- 6.0	2 °C	3.4	324	233	250
4- 6.0	2 °C	2	Not reached	Not reached	Not reached
5- 3.4	1.5 °C	4.5	25	12	10
5- 3.4	1.5 °C	3.4	219	189	204
5- 3.4	1.5 °C	2	255	251	236
5- 3.4	2 °C	4.5	238	169	174
5- 3.4	2 °C	3.4	509	359	378
5- 3.4	2 °C	2	1129	800	785
5- 8.5	1.5 °C	4.5	22	52	12
5- 8.5	1.5 °C	3.4	211	199	198
5- 8.5	1.5 °C	2	270	264	210
5- 8.5	2 °C	4.5	233	232	183
5- 8.5	2 °C	3.4	446	380	403
5- 8.5	2 °C	2	570	504	446

Table A3. Remaining carbon budgets from the Shared Socioeconomic Pathways simulations: SSP-2.45, SSP 3-7.0, 4-6.0 and 5-8.5 for 2.5, 3°C targets relative to a warming from 1850-1900.

SSP scenarios	Target	Climate sensitivity	C-only(PgC)	CN(PgC)	CNP(PgC)
2- 4.5	2.5 °C	4.5	373	321	282
2- 4.5	2.5 °C	3.4	721	567	584
2- 4.5	2.5 °C	2	Not reached	Not reached	Not reached
3- 7.0	2.5 °C	4.5	405	303	325
3- 7.0	2.5 °C	3.4	722	616	591
3- 7.0	2.5 °C	2	830	714	676
3- 7.0	3 °C	4.5	580	444	490
3- 7.0	3 °C	3.4	967	820	816
3- 7.0	3 °C	2	1118	939	942
4- 6.0	2.5 °C	4.5	380	271	303
4- 6.0	2.5 °C	3.4	670	528	542
4- 6.0	2.5 °C	2	830	658	601
4- 6.0	3 °C	4.5	545	391	454
4- 6.0	3 °C	3.4	756	703	717
4- 6.0	3 °C	2	Not reached	Not reached	Not reached
5- 8.5	2.5 °C	3.4	437	398	356
5- 8.5	2.5 °C	3.4	742	648	658
5- 8.5	2.5 °C	2	900	809	742
5- 8.5	3 °C	4.5	615	552	521
5- 8.5	3 °C	3.4	1037	875	918
5- 8.5	3 °C	2	1260	1093	1080

Appendix B: Temperature anomalies of the SSP simulations for C-only, CN and CNP
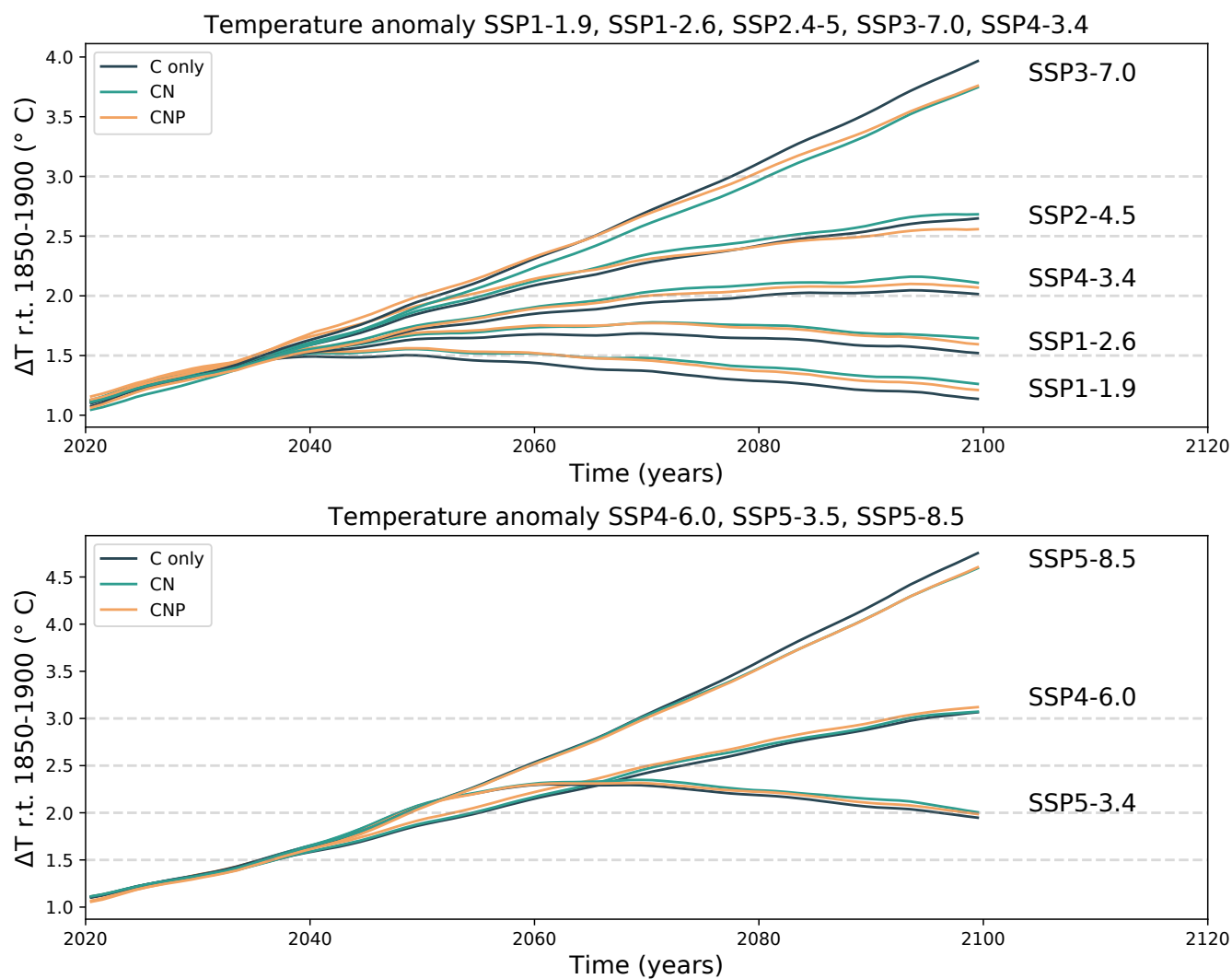
Figure B1. SSP temperature anomaly relative to 1850-1900 of C-only, CN and CNP simulations.

Appendix C: Above ground terrestrial vegetation biomass
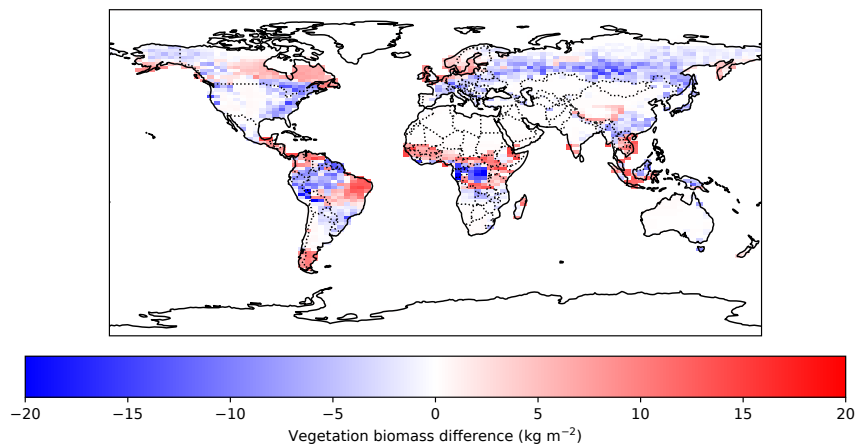
Figure C1. Above ground vegetation biomass difference between UVic ESCM CNP version 2.10 and Santoro et al. (2024) ESA CCI biomass product datasets for the years 2017-2018.

Appendix C.1 shows the above ground vegetation representation of the UVic ESCM version 2.10 with terrestrial nitrogen and phosphorus limitation. The main differences are shown to be located in tropical regions. The model both underestimates (Amazon, Borneo, Indonesian forests) and overestimated (Brazilian, Venezuelan, Colombian, central-American, Sub-Saharan and part of south east Asia forests) above-ground vegetation biomass in tropical regions in comparison with Santoro et al. (2024). However, the values estimated by the model with and without nutrients were shown to be within the range of uncertainty of literature values (Mengis et al. , 2020; De Sisto et al. , 2022).

Code and data availability.

390   The current version of the model is available from the project website: http://terra.seos.uvic.ca/model/2.10/. The exact version of the model used to produce the results used in this paper is archived on:
https://borealisdata.ca/dataset.xhtml?persistentId=doi:10.5683/SP3/GXYZKU (De Sisto , 2022).

Author contributions.

MD conducted model simulations and data analysis. MD wrote the paper and AHMD provided supervisory support.

395   *Competing interests.*

The authors declare that they have no conflict of interest.

Acknowledgements.   AHMD and MD are grateful for support from the Natural Science and Engineering Research Council of Canada Discovery Grant program and support from Compute Canada (now the Digital Research Alliance of Canada).

References

400 Achat, David Gallet-Budynek, Anne Loustau, Denis. (2016). Future challenges in coupled C–N–P cycle models for terrestrial ecosystems under global change: a review. Biogeochemistry. 131. 10.1007/s10533-016-0274-9.

Archer, D.: A data-driven model of the global calcite lysocline, Global Biogeochem. Cy., 10, 511–526, https://doi.org/10.1029/96GB01521, 1996.

Arias, P.A., N. Bellouin, E. Coppola, R.G. Jones, G. Krinner, J. Marotzke, V. Naik, M.D. Palmer, G.-K. Plattner, J. Rogelj, M. Rojas, J.

405 Sillmann, T. Storelvmo, P.W. Thorne, B. Trewin, K. Achuta Rao, B. Adhikary, R.P. Allan, K. Armour, G. Bala, R. Barimalala, S. Berger, J.G. Canadell, C. Cassou, A. Cherchi, W. Collins, W.D. Collins, S.L. Connors, S. Corti, F. Cruz, F.J. Dentener, C. Dereczynski, A. Di Luca, A. Diongue Niang, F.J. Doblas-Reyes, A. Dosio, H. Douville, F. Engelbrecht, V. Eyring, E. Fischer, P. Forster, B. Fox-Kemper, J.S. Fuglestvedt, J.C. Fyfe, N.P. Gillett, L. Goldfarb, I. Gorodetskaya, J.M. Gutierrez, R. Hamdi, E. Hawkins, H.T. Hewitt, P. Hope, A.S. Islam, C. Jones, D.S. Kaufman, R.E. Kopp, Y. Kosaka, J. Kossin, S. Krakovska, J.-Y. Lee, J. Li, T. Mauritsen, T.K. Maycock, M. Meinshausen,

410 S.-K. Min, P.M.S. Monteiro, T. Ngo-Duc, F. Otto, I. Pinto, A. Pirani, K. Raghavan, R. Ranasinghe, A.C. Ruane, L. Ruiz, J.-B. Sallée, B.H. Samset, S. Sathyendranath, S.I. Seneviratne, A.A. Sörensson, S. Szopa, I. Takayabu, A.-M. Tréguier, B. van den Hurk, R. Vautard, K. von Schuckmann, S. Zaehle, X. Zhang, and K. Zickfeld: Technical Summary. In Climate Change 2021: The Physical Science Basis. Contribution of Working Group I to the Sixth Assessment Report of the Intergovernmental Panel on Climate Change [Masson-Delmotte, V., P. Zhai, A. Pirani, S.L. Connors, C. Péan, S. Berger, N. Caud, Y. Chen, L. Goldfarb, M.I. Gomis, M. Huang, K. Leitzell, E. Lonnoy,

415 J.B.R. Matthews, T.K. Maycock, T. Waterfield, O. Yelekçi, R. Yu, and B. Zhou (eds.)]. Cambridge University Press, Cambridge, United Kingdom and New York, NY, USA, pp. 33-144. doi:10.1017/9781009157896.002. 2021.

Arora, V. K., Katavouta, A., Williams, R. G., Jones, C. D., Brovkin, V., Friedlingstein, P., Schwinger, J., Bopp, L., Boucher, O., Cadule, P., Chamberlain, M. A., Christian, J. R., Delire, C., Fisher, R. A., Hajima, T., Ilyina, T., Joetzjer, E., Kawamiya, M., Koven, C. D., Krasting, J. P., Law, R. M., Lawrence, D. M., Lenton, A., Lindsay, K., Pongratz, J., Raddatz, T., Séférian, R., Tachiiri, K., Tjiputra, J. F., Wiltshire,

420 A., Wu, T., and Ziehn, T.: Carbon–concentration and carbon–climate feedbacks in CMIP6 models and their comparison to CMIP5 models, Biogeosciences, 17, 4173–4222, https://doi.org/10.5194/bg-17-4173-2020, 2020.

Avis, C. A.: Simulating the Present-Day and Future Distribution of Permafrost in the UVic Earth System Climate Model, PhD thesis, University of Victoria, 2012.

Nico Bauer, Katherine Calvin, Johannes Emmerling, Oliver Fricko, Shinichiro Fujimori, Jérôme Hilaire, Jiyong Eom, Volker Krey, Elmar

425 Kriegler, Ioanna Mouratiadou, Harmen Sytze de Boer, Maarten van den Berg, Samuel Carrara, Vassilis Daioglou, Laurent Drouet, James E. Edmonds, David Gernaat, Petr Havlik, Nils Johnson, David Klein, Page Kyle, Giacomo Marangoni, Toshihiko Masui, Robert C. Pietzcker, Manfred Strubegger, Marshall Wise, Keywan Riahi, Detlef P. van Vuuren, Shared Socio-Economic Pathways of the Energy Sector – Quantifying the Narratives, Global Environmental Change, 42: 316-330. 2017, https://doi.org/10.1016/j.gloenvcha.2016.07.006.

Bonan, G. B. and Levis, S.: Quantifying carbon-nitrogen feedbacks in the Community Land Model (CLM4), Geophys. Res. Lett., 37,

430 2261–2282, 2010.

Bitz, C. M., Holland, M. M., Weaver, A. J., and Eby, M.: Simulating the ice-thickness distribution in a coupled, J. Geophys. Res., 106, 2441–2463, https://doi.org/10.1029/1999JC000113, 2001.

Bodirsky BL, Rolinski S, Biewald A, Weindl I, Popp A, et al. (2015) Global Food Demand Scenarios for the 21st Century. PLOS ONE 10(11): e0139201. https://doi.org/10.1371/journal.pone.0139201

435 Cox, P. M., Betts, R. A., Bunton, C. B., Essery, R. L. H., Rowntree, P. R., and Smith, J.: The impact of new land surface physics on the GCM simulation of climate and climate sensitivity, Clim. Dynam., 15, 183–203, 1999.

Cox, P. M.: Description of the TRIFFID dynamic global vegetation model, Tech. Rep. 24, Hadley Centre, Met office, London Road, Bracknell, Berks, RG122SY, UK, 2001.

De Sisto, M. L., MacDougall, A. H., Mengis, N., and Antoniello, S.: Modelling the terrestrial nitrogen and phosphorus cycle in the UVic

440 ESCM version 2.10, Geosci. Model Dev. Discuss. [preprint], https://doi.org/10.5194/gmd-2022-191, in review, 2022.

De Sisto, M. Modelling the terrestrial nitrogen and phosphorus cycle in the UVic ESCM.2022. https://doi.org/10.5683/SP3/GXYZKU, Borealis, V1.

Du, E., Terrer, C., Pellegrini, A., Ahlstrom, A., Van Lissa, C., Zhao, X., Xia, N., Wu, X. and Jackson, R.: Global patterns of terrestrial nitrogen and phosphorus limitation, Nat. Geosci. 13, 221–226, https://doi.org/10.1038/s41561-019-0530-4, 2020.

445 Eby, M., Weaver, A. J., Alexander, K., Zickfeld, K., Abe-Ouchi, A., Cimatoribus, A. A., Crespin, E., Drijfhout, S. S., Edwards, N. R., Eliseev, A. V., Feulner, G., Fichefet, T., Forest, C. E., Goosse, H., Holden, P. B., Joos, F., Kawamiya, M., Kicklighter, D., Kienert, H., Matsumoto, K., Mokhov, I. I., Monier, E., Olsen, S. M., Pedersen, J. O. P., Perrette, M., Philippon-Berthier, G., Ridgwell, A., Schlosser, A., Schneider von Deimling, T., Shaffer, G., Smith, R. S., Spahni, R., Sokolov, A. P., Steinacher, M., Tachiiri, K., Tokos, K., Yoshimori, M., Zeng, N., and Zhao, F.: Historical and idealized climate model experiments: an intercomparison of Earth system models of intermediate complexity,

450 Clim. Past, 9, 1111–1140, https://doi.org/10.5194/cp-9-1111-2013, 2013.

Eyring, V., Bony, S., Meehl, G. A., Senior, C. A., Stevens, B., Stouffer, R. J., and Taylor, K. E.: Overview of the Coupled Model Intercomparison Project Phase 6 (CMIP6) experimental design and organization, Geosci. Model Dev., 9, 1937–1958, https://doi.org/10.5194/gmd-9-1937-2016, 2016.

Fanning, A. F., Weaver, A. J. (1996). An atmospheric energy-moisture balance model: Climatology, interpentadal climate change, and

455 coupling to an ocean general circulation model. Journal of Geophysical Research, 101, 15111.

Filippelli, G.: The global phosphorus cycle, in phosphates: Geochemical, geobiological, and materials importance, Reviews in Mineralogy and Geochemistry, 391-425. 2002.

Fisher, J., Badgley, G. and Blyth, E.: Global nutrient limitation in terrestrial vegetation, Global Biogeochemical Cycles 6, https://doi.org/10.1029/2011GB004252, 2012.

460 Fowler, D., Coyle, M., Skiba, U., Sutton, M. A., Cape, J. N., Reis, S., Sheppard, L. J., Jenkins, A., Grizzetti, B., Galloway, J. N., Vitousek, P., Leach, A., Bouwman, A. F., Butterbach-Bahl, K., Dentener, F., Stevenson, D., Amann, M., Voss, M. The global nitrogen cycle in the twenty-first century. Philosophical transactions of the Royal Society of London. Series B, Biological sciences, 368(1621), 2013. https://doi.org/10.1098/rstb.2013.0164

Friedlingstein, P., Jones, M. W., O'Sullivan, M., Andrew, R. M., Bakker, D. C. E., et al.: Global Carbon Budget 2021, Earth Syst. Sci. Data,

465 14, 1917–2005, https://doi.org/10.5194/essd-14-1917-2022, 2022.

GISTEMP Team, 2023: GISS Surface Temperature Analysis (GISTEMP), version 4. NASA Goddard Institute for Space Studies. Dataset accessed 20YY-MM-DD at https://data.giss.nasa.gov/gistemp/.

Goll, D., Brovkin, V., Parida, B., Reick, C., Kattge, J., Reich, P., van Bodegom, P., and Niinemets, Ü.: Nutrient limitation reduces land carbon uptake in simulations with a model of combined carbon, nitrogen and phosphorus cycling, Biogeosciences 9, 3547–3569,

470 https://doi.org/10.5194/bg-9-3547-2012, 2012.

Goll, D., Vuichard, N., Maignan, F., Jornet-Puig, A., Sardans, J., Violette, A., Peng, S., Sun, Y., Kvakic, M., Guimberteau, M., Guenet, B., Zaehle, S., Penuelas, J., Janssens, I. and Ciais, P.: A representation of the phosphorus cycle for ORCHIDEE. Geoscientific Model Development 10, 3745-3770, doi.org/10.5194/gmd-10-3745-2017, 2017.

IPCC, 2021: Summary for Policymakers. In: Climate Change 2021: The Physical Science Basis. Contribution of Working Group I to the Sixth Assessment Report of the Intergovernmental Panel on Climate Change [Masson-Delmotte, V., P. Zhai, A. Pirani, S.L. Connors, C. Péan, S. Berger, N. Caud, Y. Chen, L. Goldfarb, M.I. Gomis, M. Huang, K. Leitzell, E. Lonnoy, J.B.R. Matthews, T.K. Maycock, T. Waterfield, O. Yelekçi, R. Yu, and B. Zhou (eds.)]. In Press.

Jones, C. D., Frölicher, T. L., Koven, C., MacDougall, A. H., Matthews, H. D., Zickfeld, K., Rogelj, J., Tokarska, K. B., Gillett, N. P., Ilyina, T., Meinshausen, M., Mengis, N., Séférian, R., Eby, M., and Burger, F. A.: The Zero Emissions Commitment Model Intercomparison Project (ZECMIP) contribution to C4MIP: quantifying committed climate changes following zero carbon emissions, Geosci. Model Dev., 12, 4375–4385, https://doi.org/10.5194/gmd-12-4375-2019, 2019.

Kanter DR, Winiwarter W, Bodirsky BL, Bouwman L, Boyer E, Buckle S, Compton JE, Dalgaard T, de Vries W, Leclere D, Leip A, Müller C, Popp A, Raghuram N, Rao S, Sutton MA, Tian H, Westhoek H, Zhang X, Zurek M. Nitrogen futures in the shared socioeconomic pathways 4. Glob Environ Change. 2020 Mar 1;61:102029. doi: 10.1016/j.gloenvcha.2019.102029. PMID: 32601516; PMCID: PMC7321850.

Kawamiya, M., Hajima, T., Tachiiri, K. et al. Two decades of Earth system modeling with an emphasis on Model for Interdisciplinary Research on Climate (MIROC). Prog Earth Planet Sci 7, 64 (2020). https://doi.org/10.1186/s40645-020-00369-5

Lu, Chaoqun Tian, Hanqin. Global nitrogen and phosphorus fertilizer use for agriculture production in the past half century: Shifted hot spots and nutrient imbalance. Earth System Science Data. 9. 181-192. 2017. 10.5194/essd-9-181-2017.

MacDougall, A. H., Avis, C. A., and Weaver, A. J.: Significant contribution to climate warming from the permafrost carbon feedback, Nat. Geosci., 5, 719–721, 2012.

MacDougall, A. H. and Knutti, R.: Projecting the release of carbon from permafrost soils using a perturbed parameter ensemble modelling approach, Biogeosciences, 13, 2123–2136, https://doi.org/10.5194/bg-13-2123-2016, 2016.

MacDougall, A.H. The Transient Response to Cumulative CO2 Emissions: a Review. Curr Clim Change Rep 2, 39–47 (2016). https://doi.org/10.1007/s40641-015-0030-6.

MacDougall, A. H., Swart, N. C., Knutti, R. The Uncertainty in the Transient Climate Response to Cumulative CO2 Emissions Arising from the Uncertainty in Physical Climate Parameters, Journal of Climate, 30(2), 813-827. 2017.

MacDougall, A. H.: Limitations of the 1% experiment as the benchmark idealized experiment for carbon cycle intercomparison in C4MIP, Geosci. Model Dev., 12, 597–611, https://doi.org/10.5194/gmd-12-597-2019, 2019.

MacDougall, A. H., Frölicher, T. L., Jones, C. D., Rogelj, J., Matthews, H. D., Zickfeld, K., Arora, V. K., Barrett, N. J., Brovkin, V., Burger, F. A., Eby, M., Eliseev, A. V., Hajima, T., Holden, P. B., Jeltsch-Thömmes, A., Koven, C., Mengis, N., Menviel, L., Michou, M., Mokhov, I. I., Oka, A., Schwinger, J., Séférian, R., Shaffer, G., Sokolov, A., Tachiiri, K., Tjiputra , J., Wiltshire, A., and Ziehn, T.: Is there warming in the pipeline? A multi-model analysis of the Zero Emissions Commitment from CO2, Biogeosciences, 17, 2987–3016, https://doi.org/10.5194/bg-17-2987-2020, 2020.

MacDougall, A. H.: Estimated effect of the permafrost carbon feedback on the zero emissions commitment to climate change, Biogeosciences, 18, 4937–4952, https://doi.org/10.5194/bg-18-4937-2021, 2021.

Matthews, H., Gillett, N., Stott, P. et al. The proportionality of global warming to cumulative carbon emissions. Nature 459, 829–832 (2009). https://doi.org/10.1038/nature08047

Matthews, H.D., Tokarska, K.B., Nicholls, Z.R.J. et al. Opportunities and challenges in using remaining carbon budgets to guide climate policy. Nat. Geosci. 13, 769–779 (2020). https://doi.org/10.1038/s41561-020-00663-3

510 McGill, W., Cole, C.: Comparative aspects of cycling of organic C, N, S, and P through soil organic matter.Geoderma 26, 267–286, 1981.

Meissner, K. J., Weaver, A. J., Matthews, H. D., and Cox, P. M.: The role of land surface dynamics in glacial inception: a study with the UVic Earth System Model, Clim. Dynam., 21, 515–537, https://doi.org/10.1007/s00382-003-0352-2, 2003.

Menge D., Hedin, L., Pacala S.: Nitrogen and Phosphorus Limitation over Long-Term Ecosystem Development in Terrestrial Ecosystems, PLOS ONE 7(8), https://doi.org/10.1371/journal.pone.0042045, 2012.

515 Mengis, N., Partanen, AI., Jalbert, J. et al. 1.5 °C carbon budget dependent on carbon cycle uncertainty and future non-CO2 forcing. Sci Rep 8, 5831. https://doi.org/10.1038/s41598-018-24241-1. 2018.

Mengis, N., Keller, D. P., MacDougall, A. H., Eby, M., Wright, N., Meissner, K. J., Oschlies, A., Schmittner, A., MacIsaac, A. J., Matthews, H. D., and Zickfeld, K.: Evaluation of the University of Victoria Earth System Climate Model version 2.10 (UVic ESCM 2.10), Geosci. Model Dev., 13, 4183–4204, https://doi.org/10.5194/gmd-13-4183-2020, 2020.

520 Myhre, G., Stocker, F., Qin, D., Plattner, G, Tignor,M., Allen, S., Boschung, J., Nauels, A., Xia, Y., Bex, V. and Midgley, P.: Anthropogenic and natural radiative forcing. Working Group I Contribution to the Intergovernmental Panel on Climate Change Fifth Assessment Report Climate Change 2013: The Physical Science Basis, Eds., Cambridge University Press. 2013.

Nakhavali, M., Mercado, L., Hartley, I., Sitch, S., Cunha, F., di Ponzio, R., Lugli, L., Quesada, C., Andersen, K., Chadburn, S., Wiltshire, A., Clark, D., Ribeiro, G., Siebert, L., Moraes, A., Schmeisk Rosa, J., Assis, R., and Camargo, J. L.: Representation of phosphorus cycle in

525 Joint UK Land Environment Simulator (vn5.5JULES-CNP), Geosci. Model Dev. Discuss., https://doi.org/10.5194/gmd-2021-403.

Brian C. O'Neill, Elmar Kriegler, Kristie L. Ebi, Eric Kemp-Benedict, Keywan Riahi, Dale S. Rothman, Bas J. van Ruijven, Detlef P. van Vuuren, Joern Birkmann, Kasper Kok, Marc Levy, William Solecki, The roads ahead: Narratives for shared socioeconomic pathways describing world futures in the 21st century, Global Environmental Change, Volume 42:169-180. 2017.https://doi.org/10.1016/j.gloenvcha.2015.01.004.

530 Pacanowski, R. C.: MOM 2 Documentation, users guide and reference manual, GFDL Ocean Group Technical Report 3, Geophys, Fluid Dyn. Lab., Princet. Univ. Princeton, NJ, 1995.

Popp, J., Lakner, Z., Harangi-Rákos, M. and Fári, M. The effect of bioenergy expansion: Food, energy, and environment, Renewable and Sustainable Energy Reviews, 32:559-578. 2014, https://doi.org/10.1016/j.rser.2014.01.056.

Reed, S. C., Townsend, A. R., Davidson, E. A., and Cleveland, C.: Stoichiometric patterns in foliar nutrient resorption across multiple scales.

535 New Phytol. 196, 173–180. 2012. doi: 10.1111/j.1469-8137.2012.04249.

J. Rogelj, D. Shindell, K. Jiang, S. Fifita, P. Forster, V. Ginzburg, C. Handa, H. Kheshgi, S. Kobayashi, E. Kriegler, L. Mundaca, R. Séférian, M. V. Vilariño, 2018, Mitigation pathways compatible with 1.5°C in the context of sustainable development. In: Global warming of 1.5°C. An IPCC Special Report on the impacts of global warming of 1.5°C above pre-industrial levels and related global greenhouse gas emission pathways, in the context of strengthening the global response to the threat of climate change, sustainable development, and

540 efforts to eradicate poverty [V. Masson-Delmotte, P. Zhai, H. O. Pörtner, D. Roberts, J. Skea, P. R. Shukla, A. Pirani, W. Moufouma-Okia, C. Péan, R. Pidcock, S. Connors, J. B. R. Matthews, Y. Chen, X. Zhou, M. I. Gomis, E. Lonnoy, T. Maycock, M. Tignor, T. Waterfield (eds.)]. In Press.

Santoro M and Cartus O 2024 ESA Biomass Climate Change Initiative (Biomass4_cci): Global datasets of forest above-ground biomass for the years 2010, 2015, 2016, 2017, 2018, 2019, 2020 and 2021, v5 NERC EDS Centre for Environmental Data Analysis

545 https://catalogue.ceda.ac.uk/uuid/02e1b18071ad45a19b4d3e8adafa2817/

Spafford, Lynsay Macdougall, Andrew H. Quantifying the probability distribution function of the transient climate response to cumulative CO2 emissions. Environmental Research Letters. 15. 10.1088/1748-9326/ab6d7b. 2020

Spafford, L. and MacDougall, A. H.: Validation of terrestrial biogeochemistry in CMIP6 Earth system models: a review, Geosci. Model Dev., 14, 5863–5889, https://doi.org/10.5194/gmd-14-5863-2021, 2021.

550 Thornton, P., Lamarque, J., Rosenbloom, N., and Mahowald, N.: Influence of carbon-nitrogen cycle coupling on land model response to CO_2 fertilization and climate variability, Global Biogeochem. Cycles 21, doi:10.1029/2006GB002868, 2007.

Selman, M., Greenhalgh, S., Diaz, R. and Sugg, Z. (2008). Eutrophication and hypoxia in coastal areas: a global assessment of the state of knowledge. WRI Policy Note. 1-6.

Seitzinger, S. P., Mayorga, E., Bouwman, A. F., Kroeze, C., Beusen, A. H. W., Billen, G., Van Drecht, G., Dumont, E., Fekete, B. M., Garnier,
555 J., and Harrison, J. A.: Global river nutrient export: A scenario analysis of past and future trends, Global Biogeochem. Cy., 24, GB0A08, doi:10.1029/2009GB003587, 2010.

Shibata, H., Branquinho, C., McDowell, W. H., Mitchell, M. J., Monteith, D. T., Tang, J., Arvola, L., Cruz, C., Cusack, D. F., Halada, L., Kopáček, J., Máguas, C., Sajidu, S., Schubert, H., Tokuchi, N., Záhora, J. Consequence of altered nitrogen cycles in the coupled human and ecological system under changing climate: The need for long-term and site-based research. Ambio, 44(3), 178–193.2015
560 https://doi.org/10.1007/s13280-014-0545-4.

Smil, V.: Phosphorus in the environment: natural flows and human interferences, Annual Review of Energy and Environment, 25,53–88, 2000.

Tokarska, Katarzyna Gillett, Nathan Arora, Vivek Lee, Warren Zickfeld, Kirsten. The influence of non-CO 2 forcings on cumulative carbon emissions budgets. Environmental Research Letters. 13. 10.1088/1748-9326/aaafdd. 2018

565 Walker, A., Beckerman, A., Gu, L., Kattge, J., Cernusak, L., Domingues, T., Scales, J., Wohlfahrt, G., Wullschleger, S. and Woodward, I.: The relationship of leaf photosynthetic traits - Vcmax and Jmax - to leaf nitrogen, leaf phosphorus, and specific leaf area: A meta-analysis and modeling study. Ecology and Evolution. 4. 2014.

Wania, R., Meissner, K., Eby, M., Arora, V., Ross, I., and Weaver, A.: Carbon-nitrogen feedbacks in the UVic ESCM, Geosci. Model Dev., 5, 1137–1160, https://doi.org/10.5194/gmd-5-1137-2012, 2012.

570 Wang, Y., Houlton, B., Field, C.: A model of biogeochemical cycles of carbon, nitrogen, and phosphorus including symbiotic nitrogen fixation and phosphatase production. Global Biogeochemical Cycles 21, 2007.

Wang, Y., Law, R., Pak, B.: A global model of carbon,nitrogen and phosphorus cycles for the terrestrial biosphere, Bio-geosciences 7, 2261–2282,doi:10.5194/bg-7-2261-2010, 2010.

Wang YP, Goll DS. Modelling of land nutrient cycles: recent progress and future development. Fac Rev. 2021 Jun 2;10:53. doi: 10.12703/r/10-
575 53. PMID: 34195692; PMCID: PMC8204758.

Wang, Yingping Goll, Daniel. (2021). Modelling of land nutrient cycles: recent progress and future development. Faculty Reviews. 10. 10.12703/r/10-53.

Weaver, A. J., Eby, M., Wiebe, E. C., Bitz, C. M., Duffy, P. B., Ewen, T. L., Fanning, A. F., Holland, M. M., MacFadyen, A., Matthews, H. D., Meissner, K. J., Saenko, O., Schmittner, A., Wang, H. X., and Yoshimori, M.: The UVic Earth System Climate Model: Model description,
580 climatology, and applications to past, present and future climates, Atmos. Ocean, 39, 361–428, 2001.

Wieder, W., Cleveland, C., Smith, W. and Todd, K.: Future productivity and carbon storage limited by terrestrial nutrient availability, Nature Geosci 8, 441–444, https://doi.org/10.1038/ngeo2413, 2015.

van Puijenbroek, P., Beusen, A. and Bouwman, A. Global nitrogen and phosphorus in urban waste water based on the Shared Socio-economic pathways, Journal of Environmental Management, 231: 446-456. 2019. https://doi.org/10.1016/j.jenvman.2018.10.048.

585 Zickfeld, K., Eby, M., Matthews, H. D., and Weaver, A. J.: Setting cumulative emissions targets to reduce the risk of dangerous climate change, Proceedings of the National Academy of Sciences, 106, 16 129–16 134, 2009.